NEOPLASIA
www.neoplasia.com

Volume 12 Number 3 March 2010 pp. 244–253 244

Prostacyclin Inhibits Non–Small Cell Lung Cancer Growth by a Frizzled 9–Dependent Pathway That Is Blocked by Secreted Frizzled-Related Protein 1[1,2]

Meredith A. Tennis*, Michelle Van Scoyk*, Lynn E. Heasley†, Katherine Vandervest*, Mary Weiser-Evans*, Scott Freeman*, Robert L. Keith*,‡, Pete Simpson*, Raphael A. Nemenoff* and Robert A. Winn*,‡

*Department of Medicine, University of Colorado Health Sciences, Denver, CO, USA; †Department of Craniofacial Biology, University of Colorado Health Sciences, Denver, CO, USA; ‡Veterans Administration Medical Center, Denver, CO, USA

Abstract

The goal of this study was to assess the ability of iloprost, an orally active prostacyclin analog, to inhibit transformed growth of human non–small cell lung cancer (NSCLC) and to define the mechanism of iloprost's tumor suppressive effects. In a panel of NSCLC cell lines, the ability of iloprost to inhibit transformed cell growth was not correlated with the expression of the cell surface receptor for prostacyclin, but instead was correlated with the presence of Frizzled 9 (Fzd 9) and the activation of peroxisome proliferator–activated receptor-γ (PPARγ). Silencing of Fzd 9 blocked PPARγ activation by iloprost, and expression of Fzd 9 in cells lacking the protein resulted in iloprost's activation of PPARγ and inhibition of transformed growth. Interestingly, soluble Frizzled-related protein-1, a well-known inhibitor of Wnt/Fzd signaling, also blocked the effects of iloprost and Fzd 9. Moreover, mice treated with iloprost had reduced lung tumors and increased Fzd 9 expression. These studies define a novel paradigm, linking the eicosanoid pathway and Wnt signaling. In addition, these data also suggest that prostacyclin analogs may represent a new class of therapeutic agents in the treatment of NSCLC where the restoration of noncanonical Wnt signaling maybe important for the inhibition of transformed cell growth.

Neoplasia (2010) 12, 244–253

Introduction

Lung cancer continues to be the leading cause of cancer death in both men and women in the United States [1]. Most lung cancers are diagnosed in former smokers, and to date, no effective treatment has been discovered for nonsurgical lung cancer. The abysmal 5-year lung cancer survival rates [2,3] underscore the need for better chemotheraputeic agents in the treatment of this disease.

Prostacyclin (PGI_2) is a naturally occurring eicosanoid that possesses anti-inflammatory and antimetastatic properties [4]. Our laboratory has demonstrated that mice with targeted overexpression of prostacyclin synthase (PGIS) in the distal lung epithelia are protected against lung tumor formation in response to chemical carcinogens or cigarette smoke [5,6]. Supplementation with iloprost (a long-acting oral PGI_2 analog) also protects against chemically induced lung carcinogenesis [7]. In fact, a recent phase 2 clinical trial provides evidence that shows iloprost to be a very effective chemopreventive agent in former smokers. However, the mechanism of iloprost's antitumorigenic effect is not well understood. Classically, the biological effects of PGI_2 are mediated through binding to a specific G protein–coupled receptor (PTGIR), which signals through G_s resulting in the elevation of cyclic adenosine monophosphate (cAMP) [8]; however, mice overexpressing PGIS that lack PTGIR, the receptor for PGIS/iloprost, are still protected against lung tumorigenesis, suggesting

Address all correspondence to: Robert A. Winn, MD, Division of Pulmonary and Critical Care Medicine, Department of Medicine, University of Colorado Denver Health Sciences Center, 12700 E 19th Ave, Aurora, CO 80045. E-mail: robert.winn@ucdenver.edu

[1]This work was supported by a VA Merit Award and the National Institutes of Health (NCI K22 CA113700).

[2]This article refers to supplementary materials, which are designated by Figures W1 and W2 and are available online at www.neoplasia.com.

Received 30 September 2009; Revised 4 January 2010; Accepted 5 January 2010

DOI 10.1593/neo.91690

signaling through other receptors [7]. In addition, the efficacy of prostacyclin analogs as chemotherapeutic agents in lung cancer has not been examined. The goal of this study was to determine the mechanism by which PGI_2/iloprost affects the growth on human non–small cell lung cancer (NSCLC) cells independent of the PTGIR membrane receptor. We report that the ability of iloprost to inhibit transformed growth is dependent on the expression of the Frizzled 9 (Fzd 9) receptor. Interestingly, iloprost, similar to Wnt 7a [9], also activates peroxisome proliferator–activated receptor-γ (PPARγ) through an ERK5-dependent pathway, suggesting that iloprost is able to mimic the effects of Wnt 7a signaling and directly signals through Fzd 9. In addition, this novel study is the first to identify an association between the Wnt 7a and prostacyclin signaling pathways in NSCLC.

Materials and Methods

Materials, Cell Culture, and Retrovirus-Mediated Gene Transfer

NSCLC lines of H358, A549, H661, H1793, H2009, H157, H460, H1334, H1703, and H2122 were cultured in RPMI 1640 medium supplemented with 10% fetal bovine serum (FBS) at 37°C in an humidified 5% CO_2 incubator. RL-65, a spontaneously immortalized, nontransformed lung epithelial cell, was cultured as previously described by Bren-Mattison [10]. BEAS-2B, another immortalized, but nontransformed lung epithelial cell line, was cultured in RPMI 1640 medium supplemented with 10% FBS at 37°C in a humidified 5% CO_2 incubator. Wi-38 was cultured in minimum essential medium with Earle salts, nonessential amino acids, glutamine, and 1 mM sodium pyruvate, supplemented with 10% FBS at 37°C in a humidified 5% CO_2 incubator. The H157-LNCX-LPCX and H157-Fzd-9 stable clones have been previously described [11,12]. H157-PTGIR stable clones were also created. The chemicals 10 μM iloprost (Cayman Chem, Ann Arbor, MI), 10 μM ciglitazone (Cayman Chem), 10 μM PGE_2 (Sigma, St. Louis, MO), 5 μM T0070907 (Cayman Chem), 25 μM PD98059 (Sigma), and 5 μM PD184352 (a generous gift from Dr. Philip Cohen, University of Dundee, Scotland) were all applied daily for each cell line used in our studies.

Quantitative Polymerase Chain Reaction

RNA was extracted from cultured cells with the RNeasy mini kit (Qiagen, Inc, Valencia, CA). Total RNA that had been extracted from the various cell lines. Aliquots of the RNA (10 μg) were converted to complementary DNA with Superscript II (Invitrogen Corp, Carlsbad, CA) and random hexamers according to the manufacturer's specifications. Primer sets for the quantitative reverse transcription–polymerase chain reaction (RT-PCR) of human Fzd 9, human and rat PTGIR, human PPARγ, human E-cadherin, and GAPDH were designed. *Rat IP/PTGIR*: For 5′ TGT CAC ATG TAC CGC CAA CAG AGA 3′, Rev 5′ ACC AGA ACT TGA GGC GTT GGA AGA 3′, *Human IP/PTGIR*: For 5′ GCC CTC CCC CTC TAC CAA 3′, Rev 5′ TTT TCC AAT AAC TGT GGT TTT TGT G 3′, *Human PPARγ*: For 5′ CAT AAT GCC ATC AGG TTT GG 3′, Rev 5′ TCA GCG GAC TCT GGA TTC AG 3′, *Human FZD9*: For 5′ AAT TTT CAT GTC ACT GGT GGT GG 3′, Rev 5′ TGC GGT AGC ACA GGG TCT G 3′, *Human E-cadherin*: For 5′CGG GAA TGC AGT TGA GGA TC 3′, Rev 5′AGGATG GTG TAA GCG ATG GC 3′, *Human GAPDH*: For 5′ GGT GTC GCT GTT GAA GTC AGA G 3′, Rev 5′ GCC AAA TAT GAT GAC ATC AAG AAG G 3′, *Mouse GAPDH*: For 5′ CGT GGA GTC TAC TGG CGT CTT CAC 3′, Rev 5′ CGG AGA TGA CCC TTT TGG C 3′. The relative quantification of real-time PCR data was determined by $\Delta\Delta C_t$. $P \leq .05$ was considered statistically significant by Student's *t*-test.

Transfections and Reporter Luciferase Assays

The reporter plasmids (PPAR-RE, PDRE, PPARα, PPARγ-gal-4, E-cadherin, Topflash, and MEF2C-gal 4), effector plasmids (Wnt 7a, Fzd 9, wild-type PPARγ, wild-type PPARδ, wild-type PPARα, soluble Frizzled-related protein-1 [sFRP1], β-catenin, PGIS, DN-MEK5, and MKK5-alpha DD), and CMV-β-gal control plasmids were transfected into cells using LipofectAmine reagent (Life Technologies, Carlsbad, CA) as previously described [12]. Small interfering RNA (siRNA) against Fzd 9 were purchased from Qiagen and used at concentrations between 50 and 75 nM. All cells were transfected with a negative control siRNA tagged with a fluorescent marker (Qiagen), which allows for an assessment of transfection efficiency.

Immunoblot Analysis

For immunoblot analysis of phospho-ERK5 (1:500; Cell Signaling, Danvers, MA), total ERK5 (1:500; Cell Signaling), phospho-p44/42 mitogen-activated protein kinase (1:1000; Cell Signaling), total p44/42 MAP kinase (1:1000; Cell Signaling), E-cadherin (1:500; BD Transduction Laboratories, San Jose, CA), β-actin (1:2000; Abcam, Cambridge, MA), β-catenin (1:1000; BD Transduction Laboratories), and Fzd 9 (1:400; Aviva Systems Biology, San Diego, CA), cell extracts were prepared in MAP kinase lysis buffer as previously described [13].

Soft Agar Colony Formation

Measurement of anchorage-independent cell growth was performed as previously described [13].

Cell Lines and cAMP Determination

Freshly isolated cell lines were resuspended in medium containing 10% fetal calf serum with 100 μM isobutylmethylxanthine (Sigma) ± 5 μM iloprost. The cells were incubated at 37°C for 45 minutes and then washed three times quickly with cold phosphate-buffered saline. The cell pellet was then lysed in cold 0.1 M HCl. Cellular cAMP content was measured using the direct cAMP kit from Assay Designs (Ann Arbor, MI). Results are reported as picomole of cAMP per milligram of protein.

Carcinogenesis Protocol and Iloprost Treatment of Mice

FVB/N mice 8 to 12 weeks of age were subjected to a single intraperitoneal injection of ethyl carbamate (Sigma) at a dose of 1 mg/g mouse weight dissolved in normal saline. To determine the ability of iloprost to prevent tumor formation, mice were fed antioxidant-free chow (AIN-76A; Test Diet, Richmond, IN) containing 3% ground iloprost tablets as described previously [5]. Iloprost or control chow was maintained for 5 weeks after the initial urethane treatment. Animals were killed 20 weeks later through pentobarbital overdose. Lungs were removed, and tumors were counted. Whole lungs from control or iloprost-fed mice were snap-frozen, and whole-cell

lysates were analyzed by Western analysis for Fzd 9 expression, as described previously.

Statistical Analysis

Experimental results are represented in graphs as means ± SEM. Data were analyzed by Student's *t*-test for comparison of two data sets using GraphPad Prism (San Diego, CA) with statistical significance at $P < .05$ and is indicated by an asterisk (*).

Results

Anchorage-Independent Growth Is Inhibited in Iloprost-Sensitive NSCLC

We assessed the effects of iloprost on anchorage-independent growth in a panel of NSCLC cell lines. Measurement of soft agar colony formation showed that iloprost was inhibitory by greater than 50% reduction in colony formation in some of the NSCLC tested

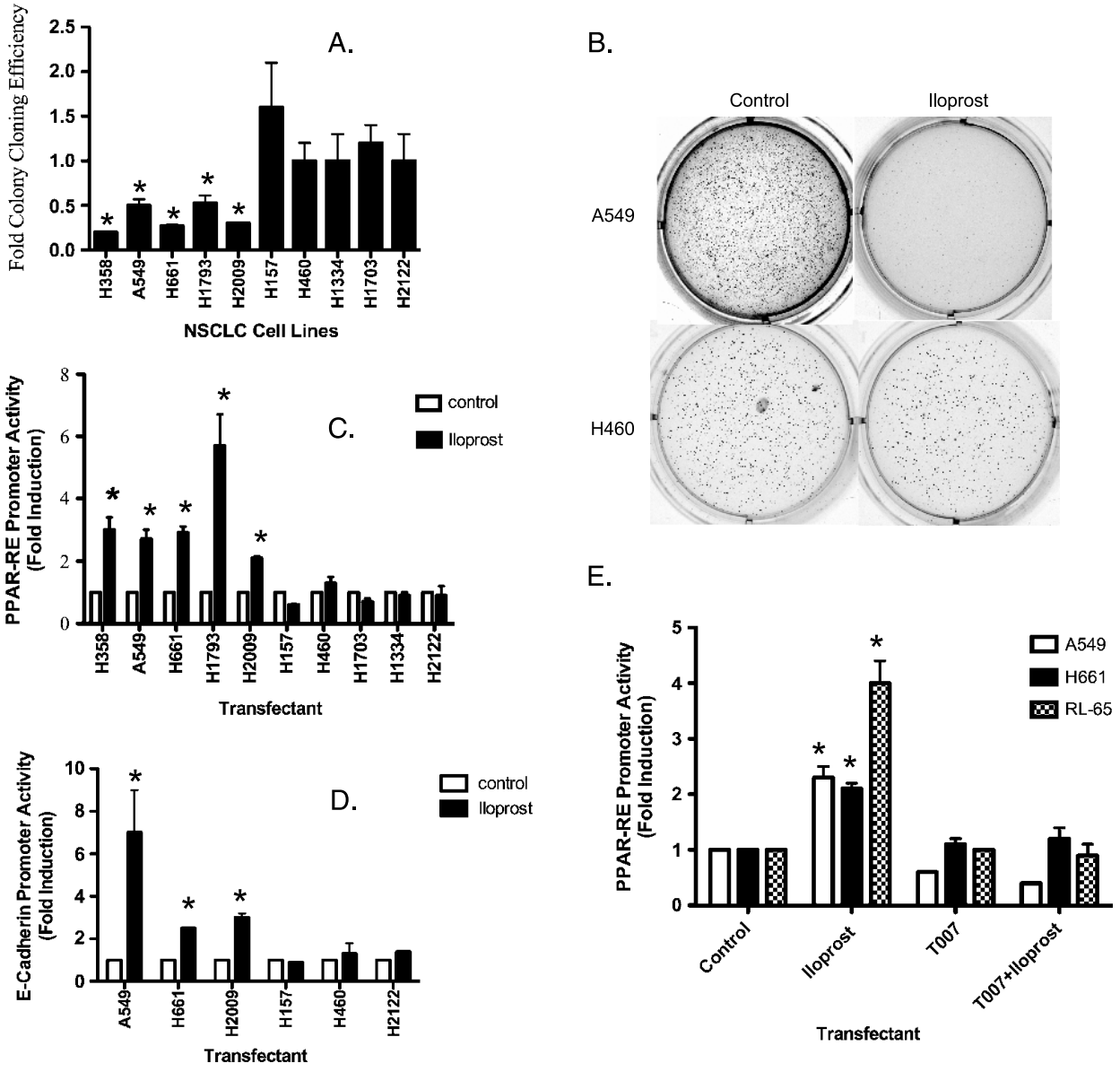

Figure 1. Iloprost inhibits anchorage-independent growth in some but not all NSCLC. (A) The indicated NSCLC cell lines were grown in soft agar in the absence or presence of 10 μM iloprost. The colonies were incubated for several weeks and subsequently counted as described in the Materials and Methods. Data are shown as mean of three independent experiments with the SEM indicated. (B) The cell line A549 is shown to be iloprost-sensitive by soft agar, whereas H460 is seen to be an iloprost-insensitive cell line. (C) Activation of PPARγ and E-cadherin is induced by iloprost. The indicated NSCLC cell lines were transiently transfected with PPAR-RE, along with CMV-β-gal to normalize for transfection efficiency. After an overnight incubation, cells were exposed for 48 hours with 10 μM iloprost. Extracts were prepared and promoter activity was determined as luciferase units normalized to CMV-β-gal. Results represent the mean of three independent experiments with the SEM indicated. (D) The indicated NSCLC cell lines were transiently transfected with E-cadherin reporter, along with CMV-β-gal to normalize for transfection efficiency and exposed for 48 hours with 10 μM iloprost. The PPARγ antagonist compound T0070907 reduces PPAR-RE activity induced by iloprost/Fzd 9. (E) The indicated cell lines were transiently transfected with PPAR-RE, or empty vector, along with CMV-β-gal to normalize for transfection efficiency. After an overnight incubation, cells were exposed for 48 hours with 10 μM iloprost and/or 5 μM T0070907.

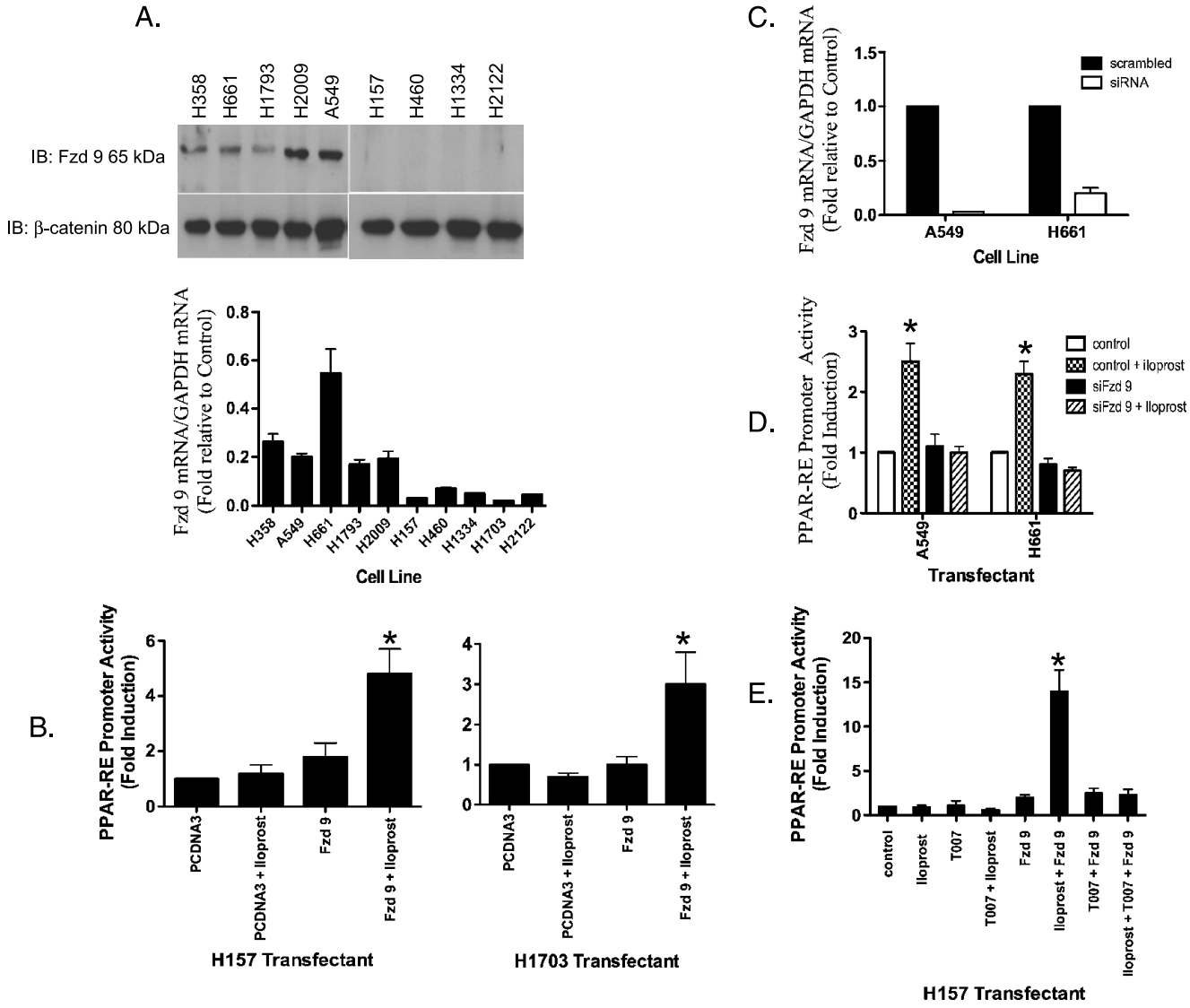

Figure 2. RNAi knockdown of Fzd 9 results in reduced PPARγ activity expression. (A) Total RNA purified from the indicated NSCLC cell lines were submitted to quantitative RT-PCR using primers specific for Fzd 9 as described under Materials and Methods. The relative mRNA abundance for Fzd 9 in the different samples was normalized to human GAPDH measured by RT-PCR in the same samples. Aliquots of extracts containing equal protein as measured by the Bradford assay from the indicated cells were resolved by SDS-PAGE and immunoblotted with antibodies to Fzd 9 (100 kDa; Aviva Systems Biology). The filters were stripped and reimmunoblotted for β-catenin (80 kDa; BD Transduction Laboratories) as a loading control. (B) The cell lines H157 and H1703 were transiently transfected with or without Fzd 9 and PPAR-RE along with CMV-β-gal to normalize for transfection efficiency. After an overnight incubation, cells were exposed for 48 hours with 10 μM iloprost. (C) siRNA knockdown of Fzd 9 was performed as described in Materials and Methods on the indicated cell lines. Total RNA purified from these cells were then submitted to quantitative RT-PCR using primers specific for Fzd 9 as previously described. The relative mRNA abundance for Fzd 9 in the different samples was normalized to human GAPDH. (D) The indicated cell lines were transiently transfected with PPAR-RE, along with CMV-β-gal to normalize for transfection efficiency. In addition, Fzd 9 was knocked down by transient siRNA expression as indicated previously. After an overnight incubation, cells were exposed for 48 hours with 10 μM iloprost. (E) The indicated cell line was transiently transfected with PPAR-RE, empty vector, or Fzd 9 along with CMV-β-gal to normalize for transfection efficiency. After an overnight incubation, cells were exposed for 48 hours with 10 μM iloprost and/or 5 μM T0070907.

(H358, A549, H661, H1793, H2009) but not in others (H157, H460, H1334, H1703, H2122; Figure 1, *A* and *B*). These results suggest that the cell lines that responded to iloprost express a receptor that the nonresponding cell lines lack. Because several studies have demonstrated frequent loss of both PGIS and PTGIR in lung cancer cell lines and primary tumors [14–16], we measured PTGIR expression by quantitative RT-PCR. Levels of PTGIR messenger RNA (mRNA) were low or undetectable in all of the NSCLC cell lines tested compared with several nontransformed lung epithelial cell lines (RL-65 and BEAS2B) and Wi-38, which was used as a positive control for PTGIR (Figure W1*A*). The NSCLC cell lines were also evaluated for their level of PPARγ expression and response to the specific PPARγ agonist ciglitazone. All the cell lines had detectable PPARγ expression as determined by quantitative RT-PCR (data not shown) and were responsive to ciglitazone as demonstrated by ciglitazone's ability to activate PPAR-RE (data not shown). To confirm the lack of functional PTGIR expression, NSCLCs were stimulated with iloprost and increases in cAMP were determined [7,17]. Iloprost failed to increase cAMP in

any of the NSCLC lines examined (Figure W2*B*). As a positive control, iloprost increased cAMP levels in H157 cells stably expressing PTGIR.

Iloprost Drives PPARγ Activation in a Subset of NSCLC and Correlates to Anchorage-Independent Growth in NSCLC Cell Lines

Data from other groups have shown that prostacylin analogs can signal through PPARs [6,18,19]. We examined the ability of iloprost to activate PPARα, PPARδ, or PPARγ in a panel of NSCLC cell lines using a PPARα-, δ-, or γ-specific reporter linked to firefly luciferase. Iloprost increased PPAR-RE activity in H358, A549, H661, H1793, and H2009, but gave no significant stimulation in H157, H460, H1334, H1703, or H2122 (Figure 1*C*). Interestingly, neither PPARα nor PPARδ was activated by iloprost in the iloprost-sensitive cell lines A549, H661, and H2009 (Figure W1*C*). We also examined E-cadherin, a downstream target of PPARγ [9,11], and discovered that iloprost similarly increased both E-cadherin reporter activity and protein expression (Figures 1*D* and W1*B*). Interestingly, iloprost increased PPAR-RE activity in several cell lines, specifically A549, H661, and RL-65, a nontransformed lung epithelial cell; this increase was completely blocked by the specific PPARγ inhibitor, T0070907 (Figure 1*E*). Thus, activation of PPARγ and E-cadherin by iloprost correlated with the inhibition of anchorage-independent growth. Iloprost did not stimulate the activation or reduction of the canonical β-catenin pathway in any of the cell lines tested (data not shown).

The Presence of Fzd 9 Is Critical for Activation of PPARγ by Iloprost

Given that most of the NSCLC cell lines lacked PTGIR (Figure W1*A*) and that iloprost did not increase PPARγ activity through cAMP (Figure W2*B*), we hypothesized that iloprost-mediated activation of PPARγ might be mediated by another seven-transmembrane spanning G protein–coupled receptor. We identified Fzd 9 as being a potential candidate receptor mediating the effects of iloprost activation of PPARγ. Quantitative RT-PCR and immunoblot of Fzd 9 mRNA and protein were detected in all cell lines in which iloprost activated PPAR-RE (H358, A549, H661, H1793, and H2009) but was absent in cells that were unresponsive to iloprost (H157, H460, H1334, H1703, and H2122; Figure 2*A*). Furthermore, quantitative RT-PCR of these NSCLC cell lines showed that the H358, A549, H661, H1793, and H2009 cells all expressed endogenous Fzd 9 but no Wnt 7a [9,12]. H460, H1334, and H2122 expressed endogenous Wnt 7a, but no Fzd 9 [9,12], and H157 and H1703 did not express either Wnt 7a or Fzd 9 [9,12]. RL-65, a spontaneously immortalized,

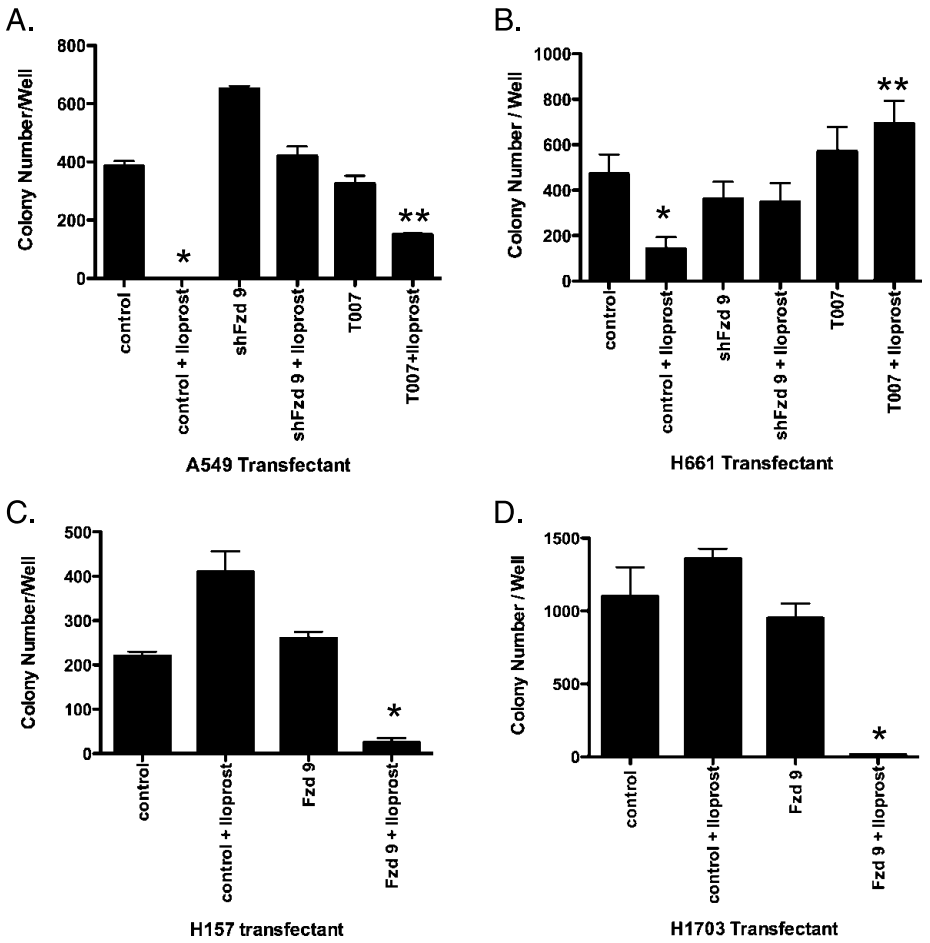

Figure 3. Fzd 9 is necessary for the effects of iloprost reversal of anchorage independent growth. (A and B) A549 and H661 cells were grown in soft agar exposed to siRNA knockdown of Fzd 9 or the PPARγ antagonist compound T0070907 at a concentration of 5 μM in the absence or presence of 10 μM iloprost. The colonies were incubated for several weeks and subsequently counted as previously described in Materials and Methods. (C and D) The H157 and H1703 cell lines encoding stable empty vector LPCX/LNCX or Fzd 9 was grown in soft agar in the absence or presence of 10 μM iloprost. The colonies were incubated for several weeks and subsequently counted through Metamorph (Downingtown, PA).

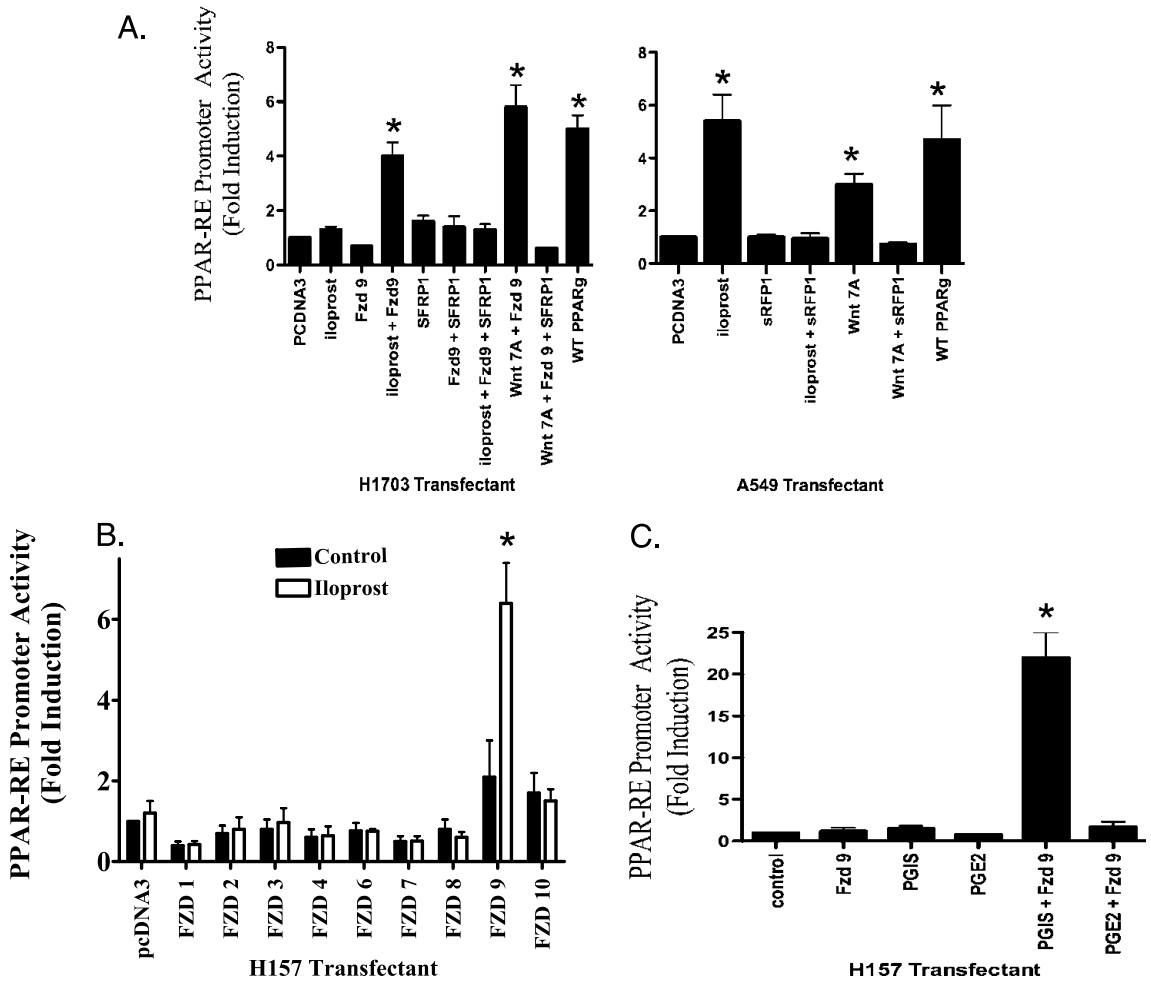

Figure 4. Iloprost and Fzd 9 are specific in its activation of PPAR-RE and is not a generalized response to all prostaglandins, the effects are also blocked by sFRP1. (A) Iloprost and Fzd 9 activate PPARγ. The A549 and H1703 cell lines were transiently transfected with the PPAR-RE, sFRP1, Fzd 9, Wnt 7a, along with CMV-β-gal to normalize for transfection efficiency. After an overnight incubation, cells were exposed for 48 hours with 10 μM iloprost. (B) The H157 cell line was transiently transfected with PPAR-RE, Fzds (1-10), along with CMV-β-gal to normalize for transfection efficiency. After an overnight incubation, cells were exposed for 48 hours with 10 μM iloprost. (C) The cell line H157 was transiently transfected with the reporter plasmid PPAR-RE and the effector plasmid PGIS, or Fzd 9, or exposed to 10 μM PGE_2. Of note, CMV-β-gal was used to normalize for transfection efficiency. The cells were incubated for 48 hours, and luciferase and β-galactosidase activities were measured. Data are presented as relative light units/milliunit of β-galactosidase activity. The results showed that the coexpression of PGIS and Fzd 9 stimulated PPAR-RE activity but not the sole expression of PGIS, Fzd 9, or PGE_2. Furthermore, the coexpression of PGE_2 and Fzd 9 similarly did not stimulate PPAR-RE activity.

nontransformed lung epithelial cell, expressed both Wnt 7a and Fzd 9. The expression of Fzd 9 or iloprost alone in both the H157 and H1703 cells (these cells lacked endogenous Wnt 7a, Fzd 9, and PTGIR) did not affect basal PPAR-RE activity, but iloprost increased PPAR-RE activity by approximately three-fold in the context of transient expression of Fzd 9 (Figure 2*B*).

We then examined the effect of silencing Fzd 9 in iloprost-sensitive cell lines. Several NSCLC lines that expressed endogenous Fzd 9 but lacked Wnt 7a and PTGIR (A549 and H661) were transfected with a siRNA to Fzd 9, resulting in significantly decreased Fzd 9 expression (Figures 2*C* and W1*B*). Silencing of Fzd 9 inhibited iloprost-mediated activation of PPARγ in all cell lines tested (Figure 2*D*). Furthermore, whereas iloprost was associated with decreased colony formation in the cell lines with endogenous Fzd 9 expression (Figure 1*A*), siRNA knockdown of Fzd 9 in theses cells resulted in no reduction of colony number on soft agar assay in the presence of iloprost (Figure 3, *A* and *B*). Conversely, we stably expressed Fzd 9 in the H157 and H1703 cell lines that lacked endogenous Fzd 9, Wnt 7a, and PTGIR proteins. We then examined the effects of the stable expression of Fzd 9 on colony formation in soft agar in the H157 and H1703 cells. In the control cells not expressing Fzd 9, iloprost did not reduce colony formation (Figure 3, *C* and *D*). Consistent with previous findings [12], stable expression of Fzd 9 alone in the H157 and H1703 cells did not affect colony formation (Figure 3, *C* and *D*). However, iloprost inhibited colony formation by approximately 90% in both the H157 and H1703 cells stably expressing Fzd 9 (Figure 3, *C* and *D*). These data indicate that iloprost and Fzd 9 have the ability to reverse anchorage-independent growth and suggest a potential tumor suppressive effect in NSCLC where iloprost can engage the Fzd 9 receptor.

Furthermore, the PPARγ antagonist compound T0070907 blocked PPAR-RE activity in H157 cells expressing Fzd 9 exposed to iloprost (Figure 2*E*). This effect was specific for Fzd 9 because overexpression of other Fzd receptors in H157 cells (1, 2, 3, 4, 6, 7, 8, and 10) failed to increase PPARγ activity (Figure 4*B*). Interestingly, the expression

of Wnt 7a in the H157 cell line did not result in further stimulation of PPAR-RE in the presence of iloprost (Figure W2*A*), supporting the idea that both iloprost and Wnt 7a interact with Fzd 9 in a similar fashion. To confirm that iloprost is mimicking the effects of PGI_2, activation of PPAR-RE was examined in H157 cells overexpressing PGIS. Overexpression of PGIS alone had no effect on PPAR-RE activity; however, transient expression of Fzd 9 significantly increased PPAR-RE activity in cells overexpressing PGIS (Figure 4*C*). Expression of PGE_2, a known protumorigenic prostacyclin family member, in the context of Fzd 9 had no effect on PPAR-RE activity (Figure 4*C*), indicating that this was not a generalized response to prostaglandins.

Expression of sFRP1 Blocks the Effect of Iloprost and Fzd 9 Activation of PPARγ

Soluble Frizzled-related proteins (sFRP) are known to block Wnt-Fzd interaction, thereby turning off the Wnt signaling pathway [20]. We investigated whether sFRP1 could also block iloprost interaction with Fzd 9. As a positive control, we coexpressed sFRP1 in the context of NSCLC cell lines expressing Wnt 7a/Fzd 9 and, as predicted, Wnt 7a/Fzd 9 was shown to have significantly reduced PPAR-RE activity in those cells exposed to sFRP1 (Figure 4*A*). More interesting, however, was that the expression of sFRP1 also blocked iloprost ability to activate PPAR-RE in cells expressing Fzd 9 (Figure 4*A*). These results suggest that there is a significant interaction between iloprost and Fzd 9.

Iloprost Activation of PPARγ Is Mediated through Activation of ERK5

We sought to determine whether iloprost activation of PPARγ involved ERK5 activation in NSCLC. Iloprost increased the MEF2C reporter activity, a marker of MEK5 activation, and the phospho-ERK5 levels five-fold in H157 cells stably expressing Fzd 9 but failed to increase phospho-ERK5 in empty vector controls (Figure 5, *A* and

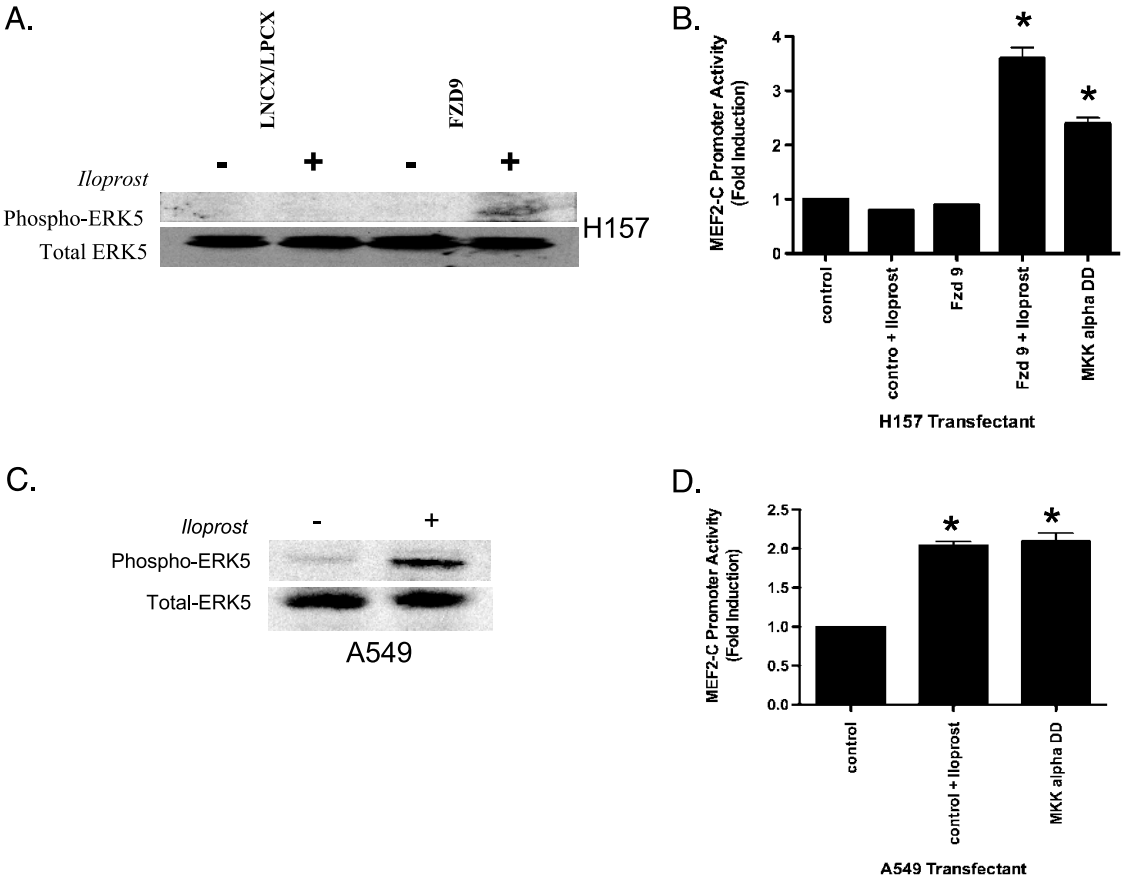

Figure 5. Iloprost and Fzd 9 induce phospho-ERK5 and MEF2C activity in NSCLC and is associated with PPARγ activity. (A) Retroviruses encoding stable empty LNCX/LPCX or Fzd 9 were used to transduce the H157 NSCLC cell line as described previously in Materials and Methods. Extracts were prepared from pooled G418 and puromycin-resistant cultures with MAPK lysis buffer, and aliquots containing 100 μg of protein were resolved on 10% polyacrylamide SDS gels, transferred to nitrocellulose, and probed with an antibody to phospho-ERK5 (115 kDa; Cell Signaling). The filters were stripped and reimmunoblotted for total ERK5 (115 kDa; Cell Signaling), which was used as a loading control protein. (B) The H157 cell line was transiently transfected with the MEF2C reporter, along with CMV-β-gal to normalize for transfection efficiency. MKK5 alpha DD was used as a positive control plasmid. After an overnight incubation, cells were exposed for 48 hours with 10 μM iloprost. (C) Retroviruses encoding empty LNCX were used to transduce the A549 NSCLC cell line as described previously in Materials and Methods. Extracts were prepared from pooled G418-resistant cultures with MAPK lysis buffer and aliquots containing 100 μg of protein were resolved on 10% polyacrylamide SDS gels, transferred to nitrocellulose, and probed with an antibody to phospho-ERK5 (115 kDa; Cell Signaling). The filters were stripped and reimmunoblotted for total ERK5 (115 kDa; Cell Signaling), which was used as a loading control protein. (D) The A549 cell line was transiently transfected with the MEF2C reporter, along with CMV-β-gal to normalize for transfection efficiency. MKK5 alpha DD was used as a positive control plasmid. After an overnight incubation, cells were exposed for 48 hours with 10 μM iloprost.

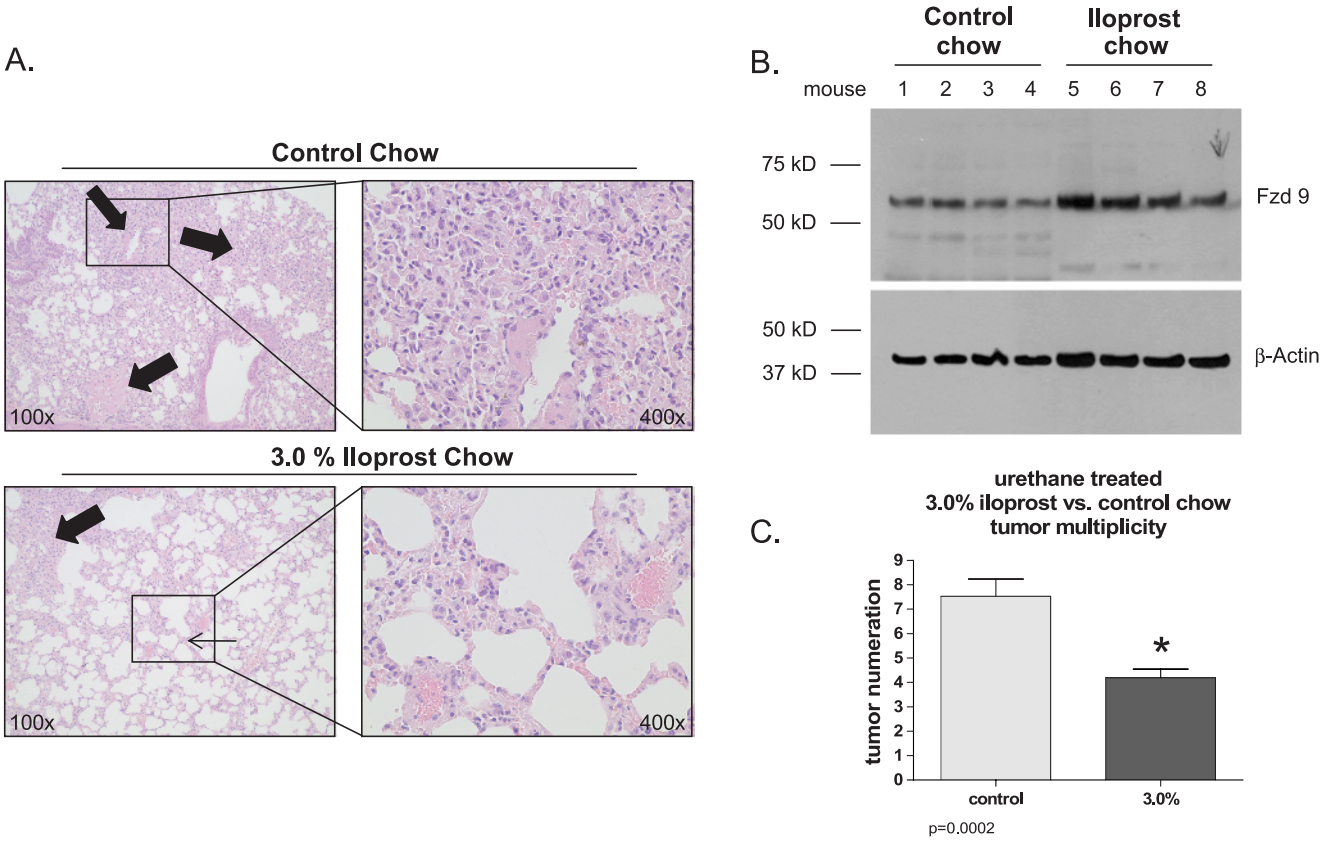

Figure 6. Iloprost treatment reduces tumor number and increases whole lung expression of Fzd 9. (A) Representative images of hematoxylin and eosin–stained urethane-treated lung tissue showing reduced tumor numbers and size in lungs from iloprost-fed mice (bottom) compared with control chow-fed mice (top). The thick arrows indicate tumor(s) in the lung and the thin arrow points out the more normal lung architecture in the mice receiving 3% iloprost chow. The right panels are higher-magnification images from the insets on the left, demonstrating the effect of iloprost on individual adenoma size. Magnifications: ×100 (left) and ×400 (right). (B) Whole lung tissue from urethane-treated mice fed normal or iloprost-impregnated chow ($n = 4$ each group) was snap-frozen, and whole-cell lysates were analyzed by Western blot analysis for Fzd 9 expression. β-Actin was used as a loading control. (C) Lungs from mice described in panel A were removed and tumors were counted. *$P = .0002$, different from control chow-fed mice.

B); levels of total ERK5 were not changed (Figure 5*A*, *bottom panels*). Similarly, A549 cells expressing endogenous Fzd 9 exposed to iloprost showed a several fold increase in p-ERK5 expression relative to the empty vector control cell lines by immunoblot and had increased induction of the MEF2C reporter activity (Figure 5*C*). In all of these cells, no significant changes in phospho-ERK1/2 levels were observed (data not shown).

To test the functional role of ERK5 in activating PPARγ, cells were treated with PD 98059, which selectively inhibits MEK1/2 and MEK5. Exposure of H157 cells to 25 μM PD98059 blocked the iloprost-mediated increase of PPAR-RE activity in cells expressing Fzd 9 (Figure W2*A*). Treatment of H157 expressing Fzd 9 with PD 184352, which selectively inhibits MEK1/2 at the concentrations used, had no effect on iloprost stimulation of PPAR-RE activity (Figure W2*A*). In addition, expression of DN-MEK5 had no effect on basal PPAR-RE activity but inhibited the activation with iloprost in the setting of Fzd 9 expression (data not shown).

Iloprost-Treated Mice Had Reduced Tumor Number and Their Sensitivity Was Associated with the Presence of Fzd 9

To determine the effect of iloprost in an *in vivo* model, FVB/N mice were maintained on control or iloprost chow for 5 weeks after urethane injection with carcinogen ethyl carbamate (urethane). The mice treated with 3% iloprost had decreased tumor numbers (3.4 ± 0.6 *vs* 7.8 ± 1.4 tumors/mouse, $P < .0002$) compared with the control mice (Figure 6, *A* and *C*). The mice receiving 3% iloprost also had a trend toward smaller tumors compared with the untreated mice.

Interestingly, the iloprost-treated mice had increased expression of Fzd 9 as detected by immunoblot (Figure 6*B*) compared with the untreated mice. Our *in vitro* experiments showed that the NSCLC cell lines that did not express Fzd 9 did not seem to have increased levels of Fzd 9 in response to iloprost (data not shown). Of note, there was no difference in the protein expression level of Wnt 7a between the treated *versus* untreated mice (data not shown). These findings suggest that the effects of iloprost's ability to reduce tumor number depend on Fzd 9 being present. The levels of PTGIR were determined to be low in these mice after urethane exposure.

Discussion

The arachidonic acid pathway and its metabolites play a central role in inflammation, pulmonary diseases, and cancer [21–23]. Elevated levels of PGE_2 have been observed in a variety of cancer, including NSCLC, leading to the use of nonsteroidal anti-inflammatory drugs as chemotherapeutic agents. In contrast, our data, as well as others, demonstrate that the levels of PGIS, PGI_2, and PTGIR are low in most NSCLC [14–16], suggesting that both PGIS and its receptor

are downregulated. Our laboratory has demonstrated that increasing PGI_2 levels through targeted overexpression of PGIS or by administration of prostacyclin analogs is chemoprotective against lung tumor formation in mice [5]. The results from a large multicenter clinical trial using iloprost in patients at risk for lung cancer seems to suggest a very favorable outcome with the use of iloprost as a chemopreventive agent in smokers. However, the chemotherapeutic potential of prostacyclin has not been investigated. Previous data have indicated that although expression of PGIS is low in most established human lung tumors [14–16], a subset of patients with detectable expression had a marked survival advantage [16]. Understanding the mechanisms whereby PGI_2 and its analogs inhibit cancer growth and progression and developing biomarkers to identify patients who may respond to PGI_2 therapy are therefore of critical importance.

From this study, we conclude that iloprost can inhibit transformed growth of a subset of NSCLC through the activation of PPARγ through an independent membrane receptor mechanism involving the Fzd 9 pathway. Work from our laboratory and by other investigators have demonstrated that PPARγ activation in NSCLC leads to growth inhibition, promotion of apoptosis, inhibition of invasiveness, and metastasis [10,11]. Moreover, PPARδ has been shown to enhance tumorigenesis in lung epithelial cells [24]. Therefore, defining the factors that are necessary for iloprost to activate PPARγ will be critical in developing this agent as a chemotherapeutic drug. Our data indicate that the expression of the G protein–coupled receptor, Fzd 9 [25–29], determines the ability of iloprost to activate PPARγ and inhibit cancer growth in NSCLC cells. Silencing of Fzd 9 expression in NSCLC cell lines that express the protein blocks the ability of iloprost to activate PPARγ and renders the cells insensitive to growth inhibition by iloprost (Figure 3, *A* and *B*). Conversely, expressing Fzd 9 in NSCLC cell lines lacking endogenous Fzd 9 seemed to sensitize the cells to growth inhibition by iloprost through a PPARγ-dependent pathway (Figure 3, *C* and *D*). Although Fzd 9 has been shown to be a receptor for Wnt 7a, and the engagement of this pathway inhibits transformed growth through ERK5-dependent activation of PPARγ [9,12], there is no existing soluble Wnt 7a protein that could be used for clinical trial. A recent study has demonstrated that prostacyclin analogs activate PPARγ through the prostacyclin receptor PTGIR [30]. Our data, however, do not support a role for PTGIR in mediating the effects of iloprost in NSCLC. All of the NSCLCs we have examined have very low to undetectable levels of PTGIR mRNA, and administration of iloprost failed to increase cAMP, an effector pathway for PTGIR (Figures W1*A* and W2*B*). Although we have not directly demonstrated iloprost binding to Fzd 9 in this current study, our data strongly suggest that this may indeed be the case as shown by sFRP1's ability to block iloprost/Fzd 9 signaling. This study is the first to demonstrate such an association between the Wnt and prostacyclin pathways. Iloprost stimulation in Fzd 9–positive cells results in the activation of ERK5 (Figure 5), as occurs with Wnt 7a stimulation, and this activation is critical for subsequent PPARγ activation.

Our data as well as others' raise the possibility that activators of PPARγ may represent an effective treatment of patients with lung cancer [9,31,32]. Thiazolinediones have been shown to reduce the risk of lung cancer in clinical trials [33], and activation of PPARγ in NSCLC cell lines has been shown to reverse the transformed phenotype in several studies [10,11,34–40]. Engagement of Fzd 9 by its ligand Wnt 7a inhibits growth of NSCLC through activation of PPARγ [9]. Whereas Wnt 7a recombinant therapy seems attractive, there is no recombinant Wnt 7a protein available for clinical use at this time. Studies using epidermal growth factor receptor inhibitors are focused on developing biomarkers to predict which patients will best respond to these agents. This study indicates that a similar strategy can be used to predict responders to iloprost by assessing their Fzd 9 status. Future clinical chemoprevention trials should determine if the expression of Fzd 9 is associated with the effects of iloprost on progression of dysplasias. However, our data indicate that Fzd 9 status may also define the utility of prostacyclin analogs as chemotherapeutic agents. Clinical trials to examine this seem to be warranted.

Acknowledgment

The authors thank Rebecca E. Schweppe for her gifts DN-MEK5, MKK5-alpha DD, and MEF2C-Luciferase reporter.

References

[1] Michaud CM, Murray CJ, and Bloom BR (2001). Burden of disease—implications for future research. *JAMA* **285**, 535–539.

[2] Jemal A, Siegel R, Ward E, Hao Y, Xu J, Murray T, and Thun MJ (2008). Cancer statistics, 2008. *CA Cancer J Clin* **58**, 71–96.

[3] Jemal A, Siegel R, Ward E, Murray T, Xu J, Smigal C, and Thun MJ (2006). Cancer statistics, 2006. *CA Cancer J Clin* **56**, 106–130.

[4] Honn KV, Cicone B, and Skoff A (1981). Prostacyclin: a potent antimetastatic agent. *Science* **212**, 1270–1272.

[5] Keith RL, Miller YE, Hoshikawa Y, Moore MD, Gesell TL, Gao B, Malkinson AM, Golpon HA, Nemenoff RA, and Geraci MW (2002). Manipulation of pulmonary prostacyclin synthase expression prevents murine lung cancer. *Cancer Res* **62**, 734–740.

[6] Keith RL, Miller YE, Hudish TM, Girod CE, Sotto-Santiago S, Franklin WA, Nemenoff RA, March TH, Nana-Sinkam SP, and Geraci MW (2004). Pulmonary prostacyclin synthase overexpression chemoprevents tobacco smoke lung carcinogenesis in mice. *Cancer Res* **64**, 5897–5904.

[7] Nemenoff R, Meyer AM, Hudish TM, Mozer AB, Snee A, Narumiya S, Stearman RS, Winn RA, Weiser-Evans M, Geraci MW, et al. (2008). Prostacyclin prevents murine lung cancer independent of the membrane receptor by activation of peroxisomal proliferator–activated receptor gamma. *Cancer Prev Res (Phila Pa)* **1**, 349–356.

[8] Narumiya S, Sugimoto Y, and Ushikubi F (1999). Prostanoid receptors: structures, properties, and functions. *Physiol Rev* **79**, 1193–1226.

[9] Winn RA, Van Scoyk M, Hammond M, Rodriguez K, Crossno JT Jr, Heasley LE, and Nemenoff RA (2006). Antitumorigenic effect of Wnt 7a and Fzd 9 in non–small cell lung cancer cells is mediated through ERK-5–dependent activation of peroxisome proliferator–activated receptor γ. *J Biol Chem* **281**, 26943–26950.

[10] Bren-Mattison Y, Van Putten V, Chan D, Winn R, Geraci MW, and Nemenoff RA (2005). Peroxisome proliferator–activated receptor-γ (PPARγ) inhibits tumorigenesis by reversing the undifferentiated phenotype of metastatic non–small-cell lung cancer cells (NSCLC). *Oncogene* **24**, 1412–1422.

[11] Wick M, Hurteau G, Dessev C, Chan D, Geraci MW, Winn RA, Heasley LE, and Nemenoff RA (2002). Peroxisome proliferator–activated receptor-γ is a target of nonsteroidal anti-inflammatory drugs mediating cyclooxygenase-independent inhibition of lung cancer cell growth. *Mol Pharmacol* **62**, 1207–1214.

[12] Winn RA, Marek L, Han SY, Rodriguez K, Rodriguez N, Hammond M, Van Scoyk M, Acosta H, Mirus J, Barry N, et al. (2005). Restoration of Wnt-7a expression reverses non–small cell lung cancer cellular transformation through frizzled-9–mediated growth inhibition and promotion of cell differentiation. *J Biol Chem* **280**, 19625–19634.

[13] Winn RA, Bremnes RM, Bemis L, Franklin WA, Miller YE, Cool C, and Heasley LE (2002). γ-Catenin expression is reduced or absent in a subset of human lung cancers and re-expression inhibits transformed cell growth. *Oncogene* **21**, 7497–7506.

[14] Hubbard WC, Alley MC, Gray GN, Green KC, McLemore TL, and Boyd MR (1989). Evidence for prostanoid biosynthesis as a biochemical feature of certain subclasses of non–small cell carcinomas of the lung as determined in established cell lines derived from human lung tumors. *Cancer Res* **49**, 826–832.

[15] Kreutzer M, Fauti T, Kaddatz K, Seifart C, Neubauer A, Schweer H, Komhoff M, Muller-Brusselbach S, and Muller R (2007). Specific components of prostanoid-signaling pathways are present in non–small cell lung cancer cells. *Oncol Rep* **18**, 497–501.

[16] Stearman RS, Dwyer-Nield L, Zerbe L, Blaine SA, Chan Z, Bunn PA Jr, Johnson GL, Hirsch FR, Merrick DT, Franklin WA, et al. (2005). Analysis of orthologous gene expression between human pulmonary adenocarcinoma and a carcinogen-induced murine model. *Am J Pathol* **167**, 1763–1775.

[17] Kiriyama M, Ushikubi F, Kobayashi T, Hirata M, Sugimoto Y, and Narumiya S (1997). Ligand binding specificities of the eight types and subtypes of the mouse prostanoid receptors expressed in Chinese hamster ovary cells. *Br J Pharmacol* **122**, 217–224.

[18] Gupta RA, Tan J, Krause WF, Geraci MW, Willson TM, Dey SK, and DuBois RN (2000). Prostacyclin-mediated activation of peroxisome proliferator–activated receptor delta in colorectal cancer. *Proc Natl Acad Sci USA* **97**, 13275–13280.

[19] Keshamouni VG, Reddy RC, Arenberg DA, Joel B, Thannickal VJ, Kalemkerian GP, and Standiford TJ (2004). Peroxisome proliferator–activated receptor-γ activation inhibits tumor progression in non–small-cell lung cancer. *Oncogene* **23**, 100–108.

[20] Kawano Y and Kypta R (2003). Secreted antagonists of the Wnt signalling pathway. *J Cell Sci* **116**, 2627–2634.

[21] Claria J (2003). Cyclooxygenase-2 biology. *Curr Pharm Des* **9**, 2177–2190.

[22] Dannenberg AJ, Lippman SM, Mann JR, Subbaramaiah K, and DuBois RN (2005). Cyclooxygenase-2 and epidermal growth factor receptor: pharmacologic targets for chemoprevention. *J Clin Oncol* **23**, 254–266.

[23] Tapiero H, Ba GN, Couvreur P, and Tew KD (2002). Polyunsaturated fatty acids (PUFA) and eicosanoids in human health and pathologies. *Biomed Pharmacother* **56**, 215–222.

[24] Pedchenko TV, Gonzalez AL, Wang D, DuBois RN, and Massion PP (2008). Peroxisome proliferator–activated receptor beta/delta expression and activation in lung cancer. *Am J Respir Cell Mol Biol* **39**, 689–696.

[25] Katanaev VL, Ponzielli R, Semeriva M, and Tomlinson A (2005). Trimeric G protein–dependent frizzled signaling in *Drosophila*. *Cell* **120**, 111–122.

[26] Malbon CC (2004). Frizzleds: new members of the superfamily of G-protein–coupled receptors. *Front Biosci* **9**, 1048–1058.

[27] Wang HY, Liu T, and Malbon CC (2006). Structure-function analysis of Frizzleds. *Cell Signal* **18**, 934–941.

[28] Wang HY and Malbon CC (2004). Wnt-frizzled signaling to G-protein–coupled effectors. *Cell Mol Life Sci* **61**, 69–75.

[29] Zeng X, Tamai K, Doble B, Li S, Huang H, Habas R, Okamura H, Woodgett J, and He X (2005). A dual-kinase mechanism for Wnt co-receptor phosphorylation and activation. *Nature* **438**, 873–877.

[30] Falcetti E, Flavell DM, Staels B, Tinker A, Haworth SG, and Clapp LH (2007). IP receptor-dependent activation of PPARγ by stable prostacyclin analogues. *Biochem Biophys Res Commun* **360**, 821–827.

[31] Keshamouni VG, Arenberg DA, Reddy RC, Newstead MJ, Anthwal S, and Standiford TJ (2005). PPAR-γ activation inhibits angiogenesis by blocking ELR+CXC chemokine production in non–small cell lung cancer. *Neoplasia* **7**, 294–301.

[32] Reddy RC, Srirangam A, Reddy K, Chen J, Gangireddy S, Kalemkerian GP, Standiford TJ, and Keshamouni VG (2008). Chemotherapeutic drugs induce PPAR-γ expression and show sequence-specific synergy with PPAR-γ ligands in inhibition of non–small cell lung cancer. *Neoplasia* **10**, 597–603.

[33] Govindarajan R, Ratnasinghe L, Simmons DL, Siegel ER, Midathada MV, Kim L, Kim PJ, Owens RJ, and Lang NP (2007). Thiazolidinediones and the risk of lung, prostate, and colon cancer in patients with diabetes. *J Clin Oncol* **25**, 1476–1481.

[34] Betz MJ, Shapiro I, Fassnacht M, Hahner S, Reincke M, and Beuschlein F (2005). Peroxisome proliferator–activated receptor-γ agonists suppress adrenocortical tumor cell proliferation and induce differentiation. *J Clin Endocrinol Metab* **90**, 3886–3896.

[35] Chang TH and Szabo E (2000). Induction of differentiation and apoptosis by ligands of peroxisome proliferator–activated receptor γ in non–small cell lung cancer. *Cancer Res* **60**, 1129–1138.

[36] Han S, Rivera HN, and Roman J (2005). Peroxisome proliferator–activated receptor-γ ligands inhibit α_5 integrin gene transcription in non–small cell lung carcinoma cells. *Am J Respir Cell Mol Biol* **32**, 350–359.

[37] Han S, Sidell N, Fisher PB, and Roman J (2004). Up-regulation of p21 gene expression by peroxisome proliferator–activated receptor γ in human lung carcinoma cells. *Clin Cancer Res* **10**, 1911–1919.

[38] Seargent JM, Yates EA, and Gill JH (2004). GW9662, a potent antagonist of PPARγ, inhibits growth of breast tumour cells and promotes the anticancer effects of the PPARγ agonist rosiglitazone, independently of PPARγ activation. *Br J Pharmacol* **143**, 933–937.

[39] Takekawa M, Maeda T, and Saito H (1998). Protein phosphatase 2Ca inhibits the human stress-responsive p38 and JNK MAPK pathways. *EMBO J* **17**, 4744–4752.

[40] Tsubouchi Y, Sano H, Kawahito Y, Mukai S, Yamada R, Kohno M, Inoue K, Hla T, and Kondo M (2000). Inhibition of human lung cancer cell growth by the peroxisome proliferator–activated receptor-γ agonists through induction of apoptosis. *Biochem Biophys Res Commun* **270**, 400–405.

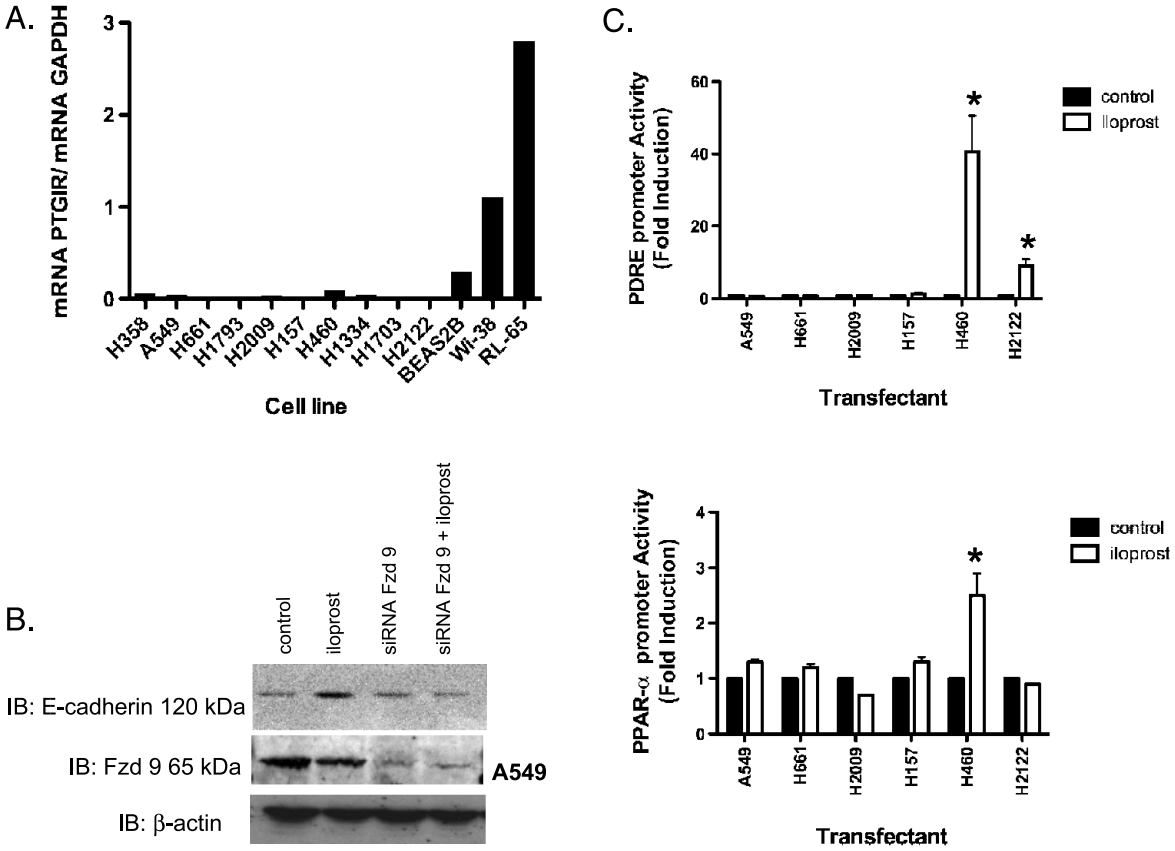

Figure W1. siRNA reduces E-cadherin expression and PTGIR is absent in NSCLC. (A) Total RNA purified from the indicated NSCLC cell lines were submitted to quantitative RT-PCR using primers specific for PTGIR as described under Materials and Methods. The relative mRNA abundance for PTGIR in the different samples was normalized to human GAPDH measured by RT-PCR in the same samples. (B) E-cadherin protein expression by iloprost and Fzd 9 are reduced by Fzd 9 siRNA knockdown. Aliquots of extracts containing equal protein as measured by the Bradford assay from the indicated cells were resolved by SDS-PAGE and immunoblotted with antibodies to E-cadherin (125 kDa; BD Transduction Laboratories) and Fzd 9 (100 kDa; Aviva Systems Biology). The filters were stripped and reimmunoblotted for β-actin (47 kDa; Abcam) as a loading control. (C) The indicated NSCLC cell lines were transiently transfected with PDRE or PPARα-luc, along with CMV-β-gal to normalize for transfection efficiency. After an overnight incubation, cells were exposed for 48 hours with 10 μM iloprost. Extracts were prepared, and promoter activity was determined as luciferase units normalized to CMV-β-gal. Results represent the mean of three independent experiments with the SEM indicated.

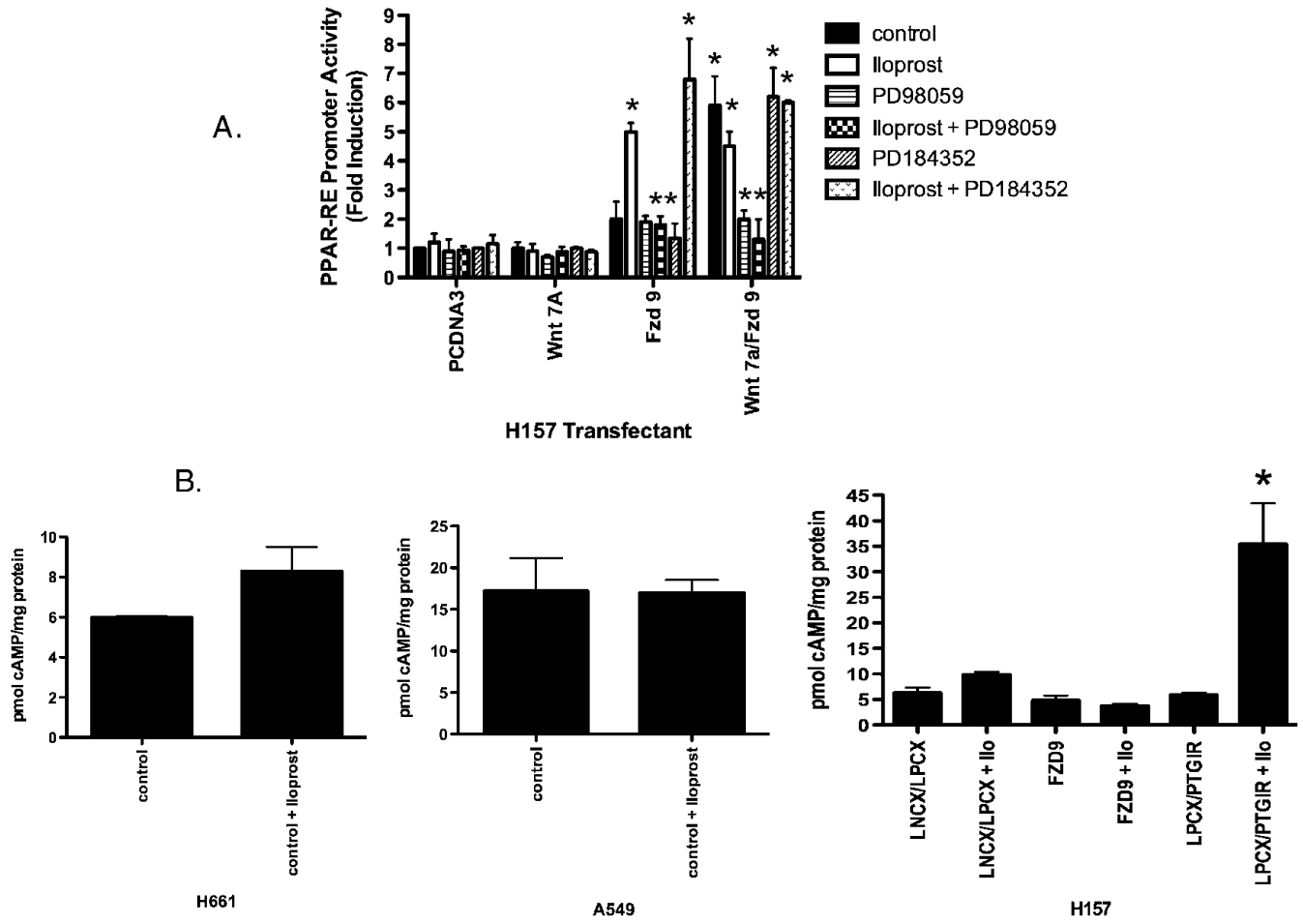

Figure W2. Iloprost and Fzd 9 do not activate PPARγ through activation of cAMP and PD98059 blocks its effect. (A) The ERK pathway inhibitor PD98059 significantly reduces PPAR-RE activity induced by both iloprost and Fzd 9 or Wnt 7a/Fzd 9, but the MEK1/2 inhibitor PD184352 has no affect the PPAR-RE activity induced by either iloprost and Fzd 9 or Wnt 7a/Fzd 9. The H157 cell line was transiently transfected with PPAR-RE, empty vector pCDNA3, Wnt 7a, Fzd 9, or both Wnt 7a/Fzd 9, along with CMV-β-gal to normalize for transfection efficiency. After an overnight incubation, cells were exposed for 48 hours with either 25 μM PD98059, 5 μM PD184352, and/or iloprost 10 μM. (B) The indicated cell lines were exposed to 10 μM of iloprost, and then cellular cAMP content was measured using the direct cAMP kit from Assay Designs. Results are reported as picomole of cAMP per milligram of protein. The H157 cell line encoding empty vector LPCX, LPCX-Fzd 9, or LPCX-PTGIR were exposed to iloprost 5 μM and measured for direct cAMP kit from Assay Designs. Results are reported as picomole of cAMP per milligram of protein.